Thermochimica Acta, 233 (1994) 257–268
Elsevier Science B.V., Amsterdam
SSDI 0040-6031(93)01471-E

Thermal decomposition of anhydrous bismuth citrate

Seham A.A. Mansour

Chemistry Department, Faculty of Science, Minia University, El-Minia (Egypt)

(Received 19 May 1993; accepted 14 June 1993)

Abstract

The thermal decomposition of anhydrous bismuth citrate in dynamic air or nitrogen has been studied. The encountered thermal events have been monitored by means of TG, DTA and DSC and the decomposition solid products analysed by IR spectroscopy and X-ray diffractometry. Non-isothermal and thermodynamic parameters have been estimated for each encountered thermal event. The results show that bismuth citrate decomposes via two events occurring exothermically in air and endothermically in nitrogen. The decomposition takes place through the formation of an intermediate composed of bismuth oxide acetate in addition to bismuth oxides in different phases. A decomposition scheme is proposed and the associated morphological and structural changes have been followed by scanning electron microscopy.

INTRODUCTION

The usual method of preparing oxide composites for electronic ceramic consists of sintering previously ground carbonates or oxides at high temperature to obtain the desired product. Since such ceramics require control of stoichiometry and reproducibility to achieve the desired electrical properties, some non-conventional solution methods of preparation could be advantageous in obtaining homogeneous mixtures of oxides. In recent years the "liquid mix technique" [1] has gained prominence for the preparation of materials for solid state devices having better physical and electrical properties than those prepared by conventional ceramic techniques, and requires no grinding or milling. In this technique, mixtures of citrates, oxalates, formates or tartrates are used to achieve homogeneous mixing on an atomic scale. To apply this technique, the mechanism of decomposition of these organic salts has to be understood both individually and in mixtures.

The thermal decomposition of several metal salts of oxalates, formates and tartrates has been studied extensively; however, similar information about citrates is scarce [1–6]. In this paper therefore, the thermal decomposition of bismuth citrate, which is widely used in medicine [3] and

for preparing bismuth oxide [6], is studied systematically. The decomposition course was followed up by IR spectroscopy, X-ray diffractometry (XRD) and scanning electron microscopy (SEM).

EXPERIMENTAL

Materials

Bismuth citrate $BiC_6H_5O_7$, was an AR grade, BDH product. It will be denoted in the text by BiCi. In view of the thermal analysis results, the material was decomposed by heating in still air at chosen temperatures for 2 h, and the products were kept dry for further analysis.

Thermal analysis

Thermogravimetry (TG), differential thermal analysis (DTA) and differential scanning calorimetry (DSC) were carried out by means of an automatically recording thermal analyzer, Schemadzu unit model 30H (Japan). TG and DTA curves were recorded in dynamic atmosphere (30 ml min^{-1}) of air at heating rates θ of 2, 5, 10 and 20°C min^{-1} and in dry nitrogen flow (30 ml min^{-1}) at 20°C min^{-1}; DSC curves were recorded in dynamic (30 ml min^{-1}) dry nitrogen atmosphere at heating rates of 2, 5, 10, 20 and 30°C min^{-1}.

Non-isothermal kinetic parameters k, A and ΔE were determined from the effect of the heating rate on the temperature (T_{max}) at which mass-variant (TG), invariant (DTA) and DSC peaks of the thermal events encountered, were maximized by adopting Ozawa methods [7, 8]. DSC data were further used to calculate the thermodynamic parameters ΔH, C_p and ΔS [9, 10]. The mathematical procedures have previously been described in detail [11].

Product analysis

Decomposition solid products were examined by IR spectroscopy, XRD and SEM.

IR spectra of BiCi and its decomposition products were recorded using a Perkin-Elmer PE 580 spectrophotometer (UK) at a resolution of 5.3 cm^{-1}, in the range 4000–200 cm^{-1}. The spectra were taken from thin ($\leq$20 mg cm^{-1}), lightly loaded (<1% by mass) KBr-based discs.

The XRD powder patterns were obtained by means of a model JSX-60

PA Jeol diffractometer (Japan) using Ni-filtered Cu Kα radiation. The diffraction patterns (I/I_0 versus d-spacing (Å), determined therefrom, were compared with the relevant ASTM standards [12].

A Jeol 35 CF scanning electron microscope was used to examine bismuth citrate and its decomposition products. Samples were mounted on the support by a clear adhesive and coated with Au/Pd. For each sample, many crystals were examined and only features identified as being typical, reproducible and significant were photographed.

RESULTS AND DISCUSSION

TG and DTA curves recorded for BiCi at 20°C min^{-1}, in dynamic atmosphere of air or nitrogen are shown in Fig. 1. In air the curves indicate that BiCi decomposes via two exothermic mass loss processes occurring in the temperature ranges 250–325°C (event I) and 360–400°C (event II), accompanied by a total loss of 42.4% of the original mass. The product is thermally stable for further heating up to 600°C, then it slowly begins to gain a small portion of mass leading to a net mass loss of 41.5% from the original. The DTA monitors two more mass-invariant endothermic

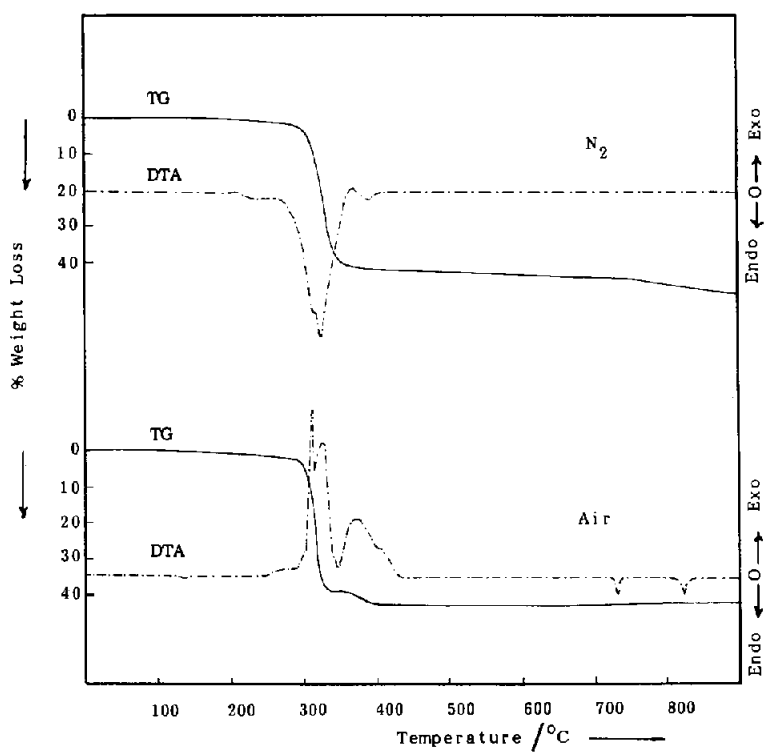

Fig. 1. TG and DTA curves recorded for BiCi at 20°C min^{-1} in dynamic (30 ml min^{-1}) atmosphere of air or dry N_2.

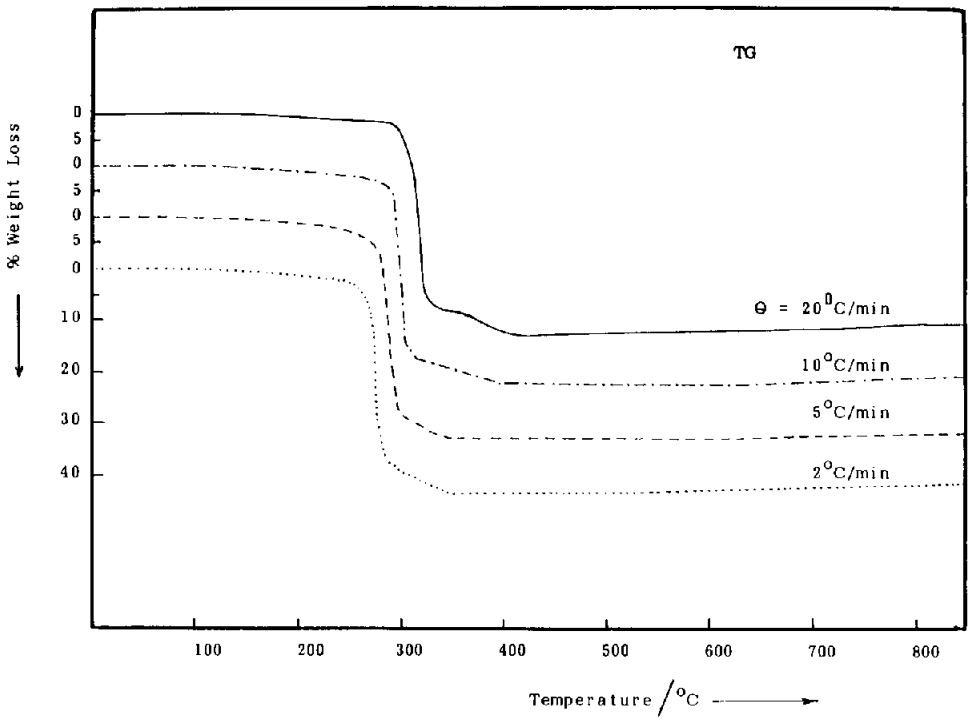

Fig. 2. TG curves recorded for BiCi at the heating rates θ indicated and in dynamic (30 ml min^{-1}) air atmosphere.

processes, maximized at 725°C (event III) and 825°C (event IV). Figure 2 shows the effect of the heating rate on the thermal behaviour of BiCi in air.

Characterization of the thermal events

Event I

Figure 1 shows that in air, event I is an exothermic mass loss process, maximized at 314°C. The IR spectrum of the decomposition product at 280°C (Fig. 3) shows a marked reduction in the intensities of the bands displayed by the parent citrate. The spectrum also reveals reduction of the carboxylate band at 1450 cm^{-1} and of the OH stretching band at 3470 cm^{-1}. This latter band completely disappears in the spectrum of the decomposition product at 300°C (Fig. 3) which displays absorption bands at 635, 507, 445, 385 and 345 cm^{-1}, assigned to bismuth oxides [13]. The XRD pattern of the decomposition product at 300°C (Fig. 4) reveals the disappearance of the diffraction lines of the original citrate. The pattern exhibits the lines of Bi_2O_3 (α-phase (ASTM card no. 27–53) and β-phase (ASTM card no. 29–236)) as well as the lines of bismuth oxide acetate (ASTM card no. 14-800) in addition to the lines of BiO (ASTM card no. 27–54). These

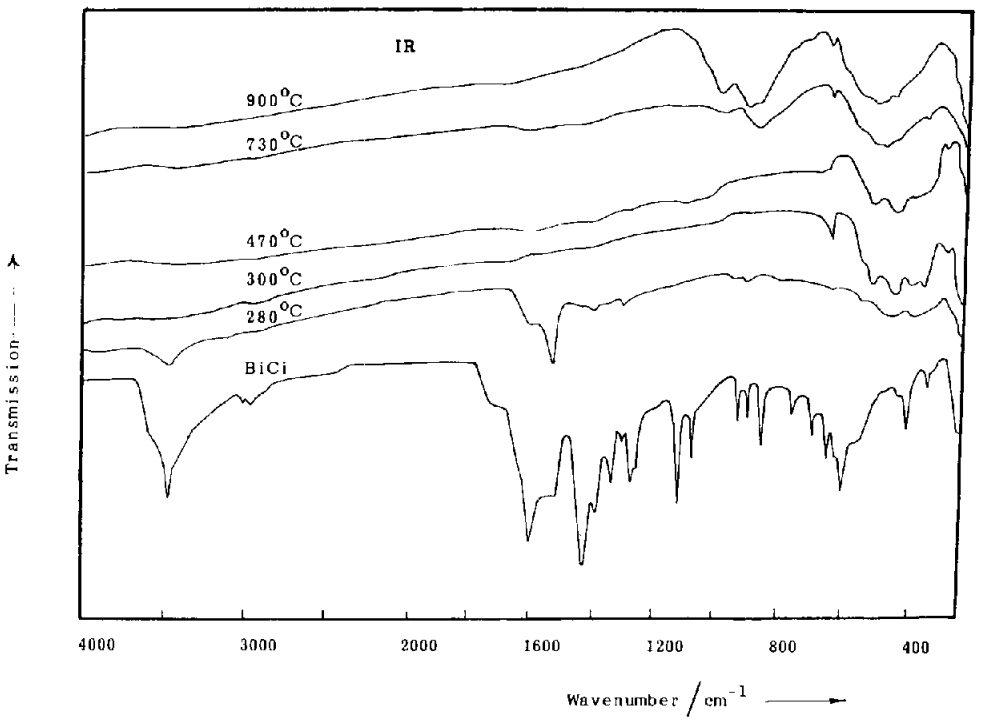

Fig. 3. IR spectra of the parent BiCi and its decomposition products at the temperatures indicated for 2 h in still air.

results suggest that event I involves the formation of an intermediate composed of all these compounds as represented by the reaction

$$4BiC_6H_5O_7 \longrightarrow BiO + Bi_2O_3 + BiO(CH_3COO)$$

$-17H$

$-21O$

$-22C$ (as CO and CO_2)

The observed mass loss accompanying this event amounts to 38.6% which is fairly close to the calculated value (38.7%) for the proposed transformation according to the above equation. The pyrolysis of the carbon produced from this reaction by the atmospheric oxygen is responsible for the exothermic nature of this event. However, results for the thermal decomposition of BiCi in dynamic dry nitrogen atmosphere (Fig. 1) show this event to occur endothermically. This confirms the role of the atmospheric oxygen in modifying the nature of this decomposition process from endothermic to exothermic in flowing air. Furthermore, the DSC curves in dry nitrogen atmosphere (Fig. 5) show the endothermic response of this process. The corresponding activation energy ΔE for this event was found to be 105 kJ mol^{-1} in air (Table 1) and 39 kJ mol^{-1} in nitrogen (Table 2).

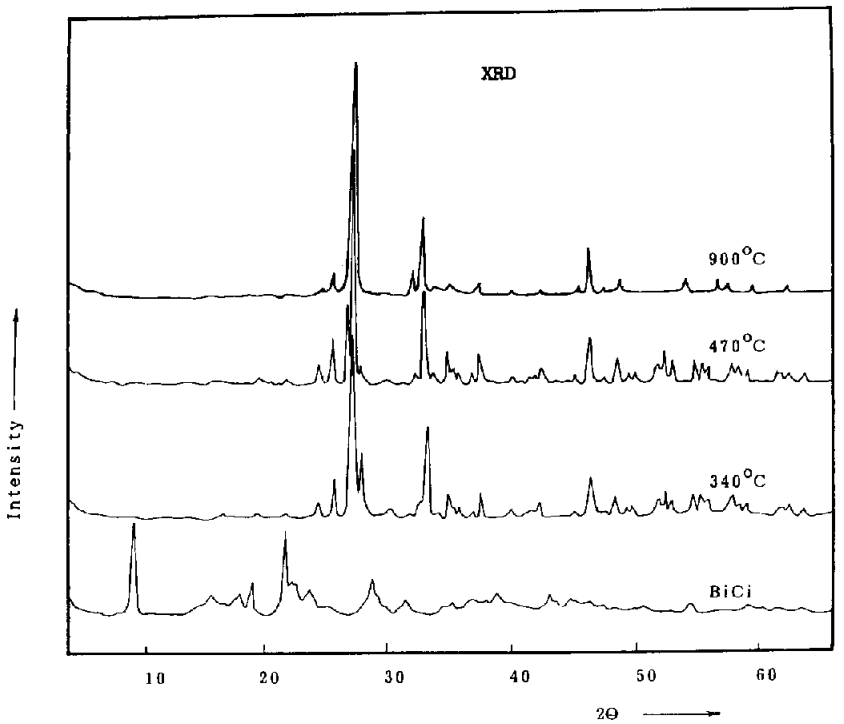

Fig. 4. XRD powder diffractograms of the parent BiCi and its decomposition product at the temperatures indicated for 2 h in still air.

Event II

Figure 1 shows that event II takes place in air exothermically in the temperature range 355–400°C, with a maximum at 370°C. By the end of this event, the total mass loss was found to be 42.4%. The IR spectrum of the decomposition product at 470°C (Fig. 3) displays only the characteristic bands of bismuth oxides. Furthermore, the diffractogram of this decomposition product (Fig. 4) exihibits only the patterns of BiO and Bi_2O_3 in both phases. These results suggest that event II may involve the reaction

$$BiO + Bi_2O_3 + BiO(CH_3COO) \xrightarrow[-3H,\ -(3/2)O]{-2C} BiO + (3/2)Bi_2O_3$$

The associated mass loss (3.8% with respect to the parent salt) is close to that corresponding to the above equation (about 3.2%).

Again this event occurred endothermically under nitrogen flow (Fig. 1), while the pyrolysis process in air disguised its thermic nature transforming it into an exothermic one. The associated activation energy ΔE was found to be 95 kJ mol^{-1} in air (Table 1) and 29 kJ mol^{-1} in nitrogen (Table 2). This

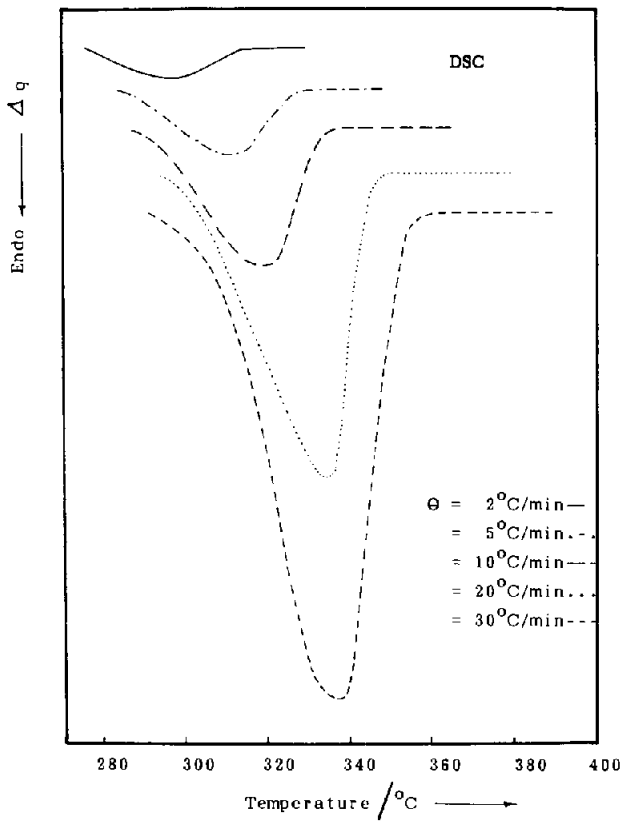

Fig. 5. DSC curves recorded for BiCi at the heating rates θ indicated in dynamic (30 ml min^{-1}) atmosphere of dry nitrogen.

event is accompanied by a decrease in ΔS and C_p indicating that it is associated with a decrease in disorder.

It is worth noting that the product slowly gains small portion of mass (about 0.9%). Such an observed mass increase terminates at 850°C. The IR spectra of the decomposition product at 730 and 900°C (Fig. 3) display a marked sharpness in the observed bands of Bi_2O_3 [13]. Moreover, the XRD pattern of the decomposition product at 900°C exhibits the characteristic lines of Bi_2O_3 (Fig. 4). Hence, it could be concluded that the increase in product mass upon further heating in air is clearly attributable to the oxidation of its BiO content by atmospheric oxygen giving rise to Bi_2O_3 as a final decomposition product. In fact the net mass loss (41.4%) is very close to that anticipated for the transformation

$$2(BiC_6H_5O_7) \rightarrow Bi_2O_3$$

In contrast, further heating in flowing nitrogen resulted in continuous

TABLE 1

Non-isothermal kinetic parameters of the thermal events occurring throughout the decomposition course of BiCi in dynamic air [a]

Thermal event	ΔE/kJ mol^{-1}	k/min^{-1}	log A	$\Delta T/T$
I	105	0.25	8	exo
II	95	0.35	16	exo
III	28			endo
IV	31			endo

[a] The kinetic parameters for thermal events I and II were calculated from TG data whereas for events III and IV, DTA data were used.

TABLE 2

Non-isothermal kinetic and thermodynamic parameters of the thermal events encountered throughout the decomposition course of BiCi in dry N_2 atmosphere, derived from the DSC curves recorded at 10°C min^{-1}

Thermal event	Temperature range/°C	ΔE/kJ mol^{-1}	k/min^{-1}	ln A	ΔH/kJ mol^{-1}	C_p/J g^{-1}	ΔS/J K^{-1} g^{-1}
I	288–336	39	0.13	58	46.3	2.41	0.198
II	344–358	29	0.09	32	39.8	0.32	0.007

loss in the product mass, which could be due to an increase in the product metal content either in the metallic phase or as oxygen deficient oxides. Further studies are needed to identify the composition of the decomposition products under nitrogen flow.

Events III and IV

The DTA curve (Fig. 1) indicates the occurrence of two endothermic mass-invariant events III and IV with maxima at 725 and 825°C, respectively. These two events are most probably due to the melting of α-Bi_2O_3 and β-Bi_2O_3, respectively [14]. The associated activation energies ΔE were found to be 28 and 31 kJ mol^{-1} for events III and IV, respectively (Table 1).

Electron microscopic examination

SEM studies of the parent BiCi revealed that it was composed of coherent aggregates of irregular shape composed of crystallites of irregular shape, and wide size range (Fig. 6(a)). Heating BiCi to 280°C resulted in a

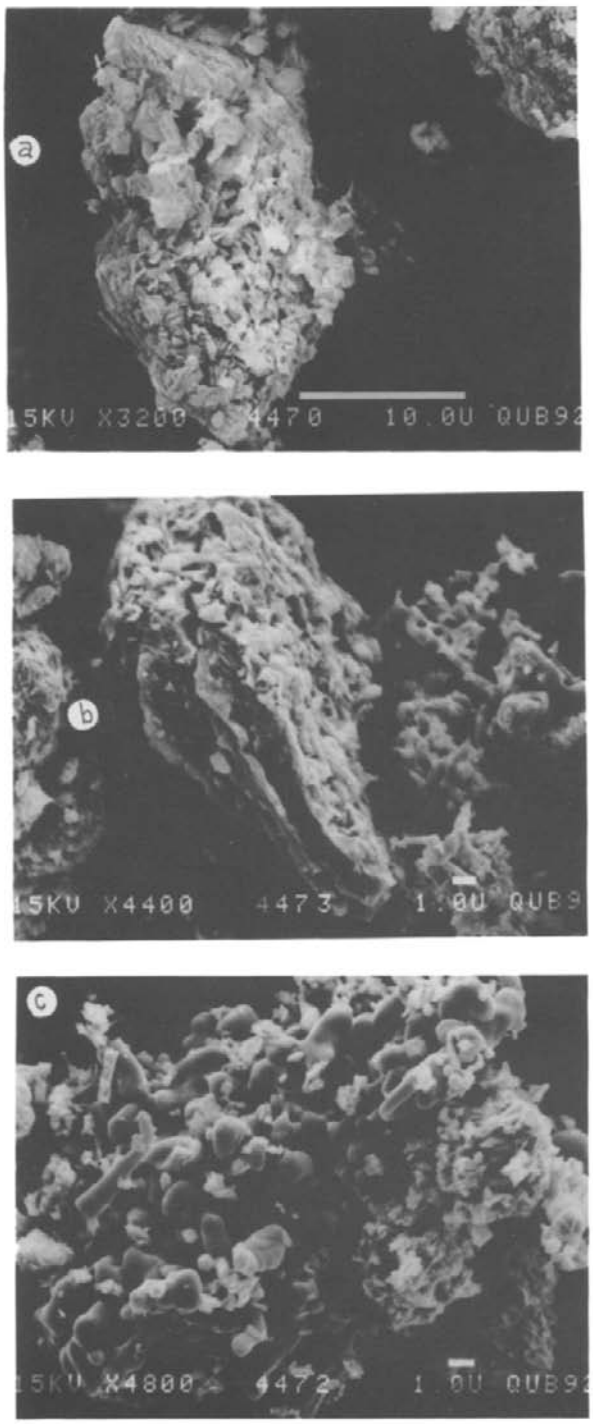

Fig. 6. Scanning electron micrographs of (a) the parent BiCi, (b) the decomposition product at 280°C and (c) the decomposition product at 300°C.

marked change in the morphology and structure of these aggregates. The most important features were the loss of coherency and the appearance of parallel cleaves as seen in Fig. 6(b). These features were exaggerated at 300°C (Fig. 6(c)) where the electron micrographs of the decomposition product revealed the formation of new crystallites with smooth rounded surfaces, assigned most probably to Bi_2O_3. The micrograph also reveals the presence of more than one crystal shape. This is in accord with the thermoanalytical results (TG, IR spectroscopy and XRD), which revealed the formation of a composite intermediate at 300°C containing bismuth oxides and bismuth oxide acetate.

Examination of the decomposition product at 470°C showed a marked growth in the Bi_2O_3 crystallites and the material retained its coherency (Fig. 7(a)). It is clear that the Bi_2O_3 formed is crystalline with rounded smooth

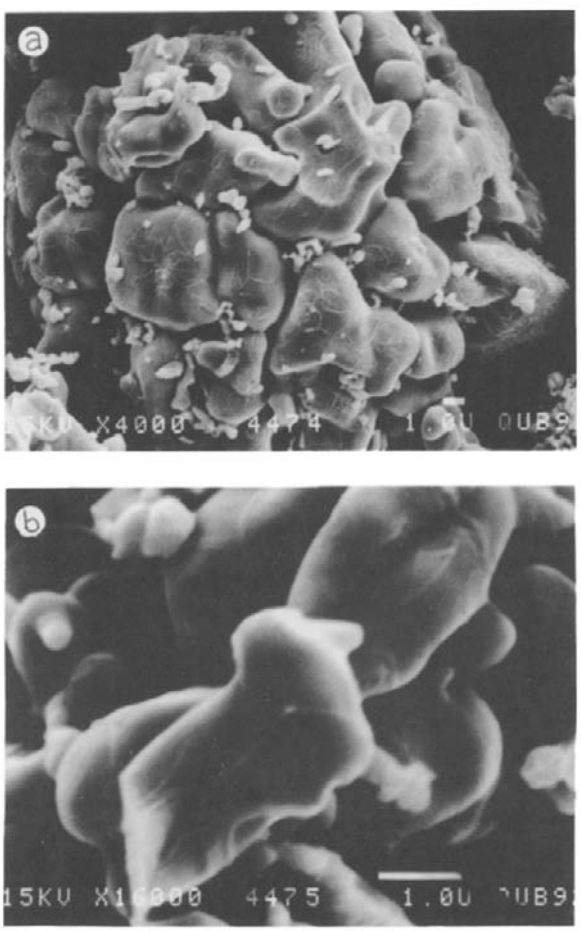

Fig. 7. Scanning electron micrographs of the decomposition product at 470°C, showing (a) signs of coherency in addition to (b) the formation of slightly wrinkled crystallites of smooth surface.

surfaces which exhibit small portions of wrinkles (Fig. 7(b)). A minute portion of another crystal shape appeared in the micrograph which decreased and then disappeared at higher temperatures (about 900°C). These results agree with those of XRD and IR analyses, which indicated the formation of different phases of Bi_2O_3 (α and β) at 470°C in addition to a minute amount of BiO which transformed into Bi_2O_3 at high temperature.

CONCLUSIONS

(1) The thermal decomposition of BiCi in dynamic air, involves the pathways

$$4BiC_6H_5O_7 \xrightarrow{I} BiO + Bi_2O_2 + BiO(CH_3COO) \xrightarrow{II}$$

$$BiO + (3/2)Bi_2O_3 \rightarrow 2Bi_2O_3$$

The Roman numerals indicate the encountered thermal events.

(2) The resultant Bi_2O_3 was found to exhibit α and β phases which melted at 725°C and 825°C, respectively.

(3) The decomposition processes were endothermic in nitrogen while in air they took place exothermically.

(4) The morphological and structural changes occurring throughout the decomposition course were followed by SEM the results of which were found to be in accord with IR and XRD data.

ACKNOWLEDGEMENTS

It is a pleasure to thank the Queen's University of Belfast, particularly the staff of the electron microscope for assistance in obtaining the electron micrographs. Thanks are also due to the Egyptian Government for the grant of a fellowship.

REFERENCES

1 A. Srivastava, P. Singh, V.G. Gunjikar and C.I. Jose, Thermochim. Acta, 76 (1984) 249.
2 F. Smeets, U.S. Patent 3,586,715 (1966).
3 A. Radecki and M. Wesolowski, Thermochim. Acta, 17 (1976) 217.
4 J. Mastowska, J. Therm. Anal., 29 (1984) 895.
5 J. Mastowska, M. Bielawski and A. Baranowska, Thermochim. Acta, 92 (1985) 235.
6 A. Srivastava, V.G. Gunjikar and A.P.B. Sinha, Thermochim. Acta, 117 (1987) 201.
7 T. Ozawa, J. Therm. Anal., 2 (1970) 301.
8 T. Ozawa, J. Therm. Anal., 9 (1976) 369.
9 K.F. Baker, Du Pont Instruments, Thermal Analysis Application Brief, No. TA-53.
10 C. Heald and A.C.K. Smith, Applied Physical Chemistry, Macmillan, London, 1982, pp. 20–40.
11 S.A.A. Mansour, Thermochim. Acta, 228 (1993) 155.

12 W. Frank et al. (Eds.), Powder Diffraction File for Inorganic Phase, Int. Center for Diffraction Data, Philadelphia, PA, 1981.
13 N.T. McDevitt and W.L. Baun, Spectrochim. Acta, 20 (1964) 799.
14 R.C. Weast (Ed.), CRC Handbook of Chemistry and Physics, CRC Press, Boca Raton, FL 62nd edn., 1981.